

and surrounding metal that formed later [1,2]. Here we report spatially resolved trace-element concentration measurements in metal grains in HH 237, for the platinum group elements (PGEs) and the moderately volatile siderophile elements Cu, Ga, and Ge, to further constrain the origin of bencubbinite metal.

**Experiments:** The section HH 237 AMNH 4956-4 was mapped using a CAMECA SX100 electronprobe, and compositional profiles of Cr, Fe, Co, and Ni were determined. Large (>100  $\mu\text{m}$ ) chemically zoned metal grains were selected for trace-element microanalysis by LA-ICP-MS.

A CETAC LSX-200 laser ablation peripheral was used with a magnetic sector ICP mass spectrometer, the Finnigan Element<sup>TM</sup>. It was first confirmed that the PGE distributions in HH 237 zoned metal mimics those in QUE 94411 [2]. To enhance sensitivity for the measurement of moderately volatile elements, a larger laser-ablated sample size was then used. Each point on the sample was analyzed with 100-pulse laser bursts; the laser-ablated pit produced was approximately 50  $\mu\text{m}$  in diameter and 35  $\mu\text{m}$  deep. A series of analyses were performed across each grain in ~50- $\mu\text{m}$  steps. The isotopes monitored were <sup>53</sup>Cr, <sup>57</sup>Fe, <sup>59</sup>Co, <sup>60</sup>Ni, <sup>63</sup>Cu, <sup>69</sup>Ga, <sup>74</sup>Ge, <sup>75</sup>As, <sup>95</sup>Mo, <sup>101</sup>Ru, <sup>103</sup>Rh, <sup>105</sup>Pd, <sup>118</sup>Sn, and <sup>121</sup>Sb. Instrumental sensitivity factors for each isotope were determined from external standards [3]. Precision of the LA-ICP-MS measurements was typically 5% (1 $\sigma$ ).

**Results and Discussion:** Refractory siderophiles display a radial gradient in a representative HH 237 zoned grain that mimics that of Ni and Co, similar to that observed in QUE 94411 [2]. Palladium, which has similar volatility to Fe, shows no radial zoning and is enriched by a constant factor of ~1.2. Volatile siderophiles are depleted with respect to Fe in the grain. Chromium is radially zoned with a minimum Fe, CI-normalized abundance at the center of about 0.1. Copper is depleted by a factor of 500 at the grain core, and displays a much steeper concentration gradient than the other elements. Germanium is depleted by at least a factor of 250, but is less depleted at the rim. The remaining elements, Ga, As, Sn, and Sb, are all below current detection limits throughout the HH 237 zoned grain. These depletions in part reflect the depletions measured in bulk bencubbinites [4].

The volatile depletion in the grain core supports the conclusion that these grains originated as high-temperature condensates [1,2]. The steep Cu and Ge gradients at the rim allow constraints to be placed on the extent of diffusion into the grain, and the rim composition places a lower limit on the temperature of isolation of the grain from the condensing gas.

**References:** [1] Meibom A. et al. (1999) *JGR*, 104, 22053–22059; Weisberg M. K. et al. (2000) *LPS XXXI*, Abstract #1466; Meibom et al. (2000) *Science*, 288, 839–841. [2] Campbell A. J. et al. (2000) *LPS XXXI*, Abstract #1490; Campbell A. J. et al. (2000) *GCA*, submitted. [3] Campbell A. J. and Humayun M. (1999) *LPS XXX*, Abstract #1974. [4] Weisberg M. K. et al. (2000) *MAPS*, submitted; Campbell A. J. and Humayun M., this volume.

**NEAR SHOEMAKER'S NEW VIEW OF EROS: IMPACT PROCESSES AND "SPACE WEATHERING."** C. R. Chapman<sup>1</sup> and the NEAR MSINIS Team, <sup>1</sup>Southwest Research Institute, Suite 426, 1050 Walnut Street, Boulder CO 80302, USA (cchapman@boulder.swri.edu).

**Introduction:** *NEAR Shoemaker's* new perspectives on Eros are coming into focus. Here we consider two related aspects of Eros in the context of long-standing issues in asteroid science: (1) its impact history and (2) the long-standing S-type conundrum [1]. Eros' composition is apparently like that of L or LL chondrites, based on X-ray data [2], consistent with its IR spectral reflectance and with the spatial homogeneity of its spectral properties in the hemisphere observed by MSI and NIS [3]. It is premature, however, to conclude that the S-type issue has been resolved. Not only is Eros merely a single example of an S-type — a large, heterogeneous taxonomic class — but *NEAR Shoemaker's* images have revealed truly puzzling geology.

**Crater Populations:** The largest crater is 5.5 km across, although the "saddle" more than twice as big may be of impact origin, too. The proximity of the most prominent compressional ridge to the saddle could suggest that both formed when two large objects accreted into the present-day configuration of Eros, perhaps in the aftermath of the collisional break-up of Eros' precursor body. Unprecedented evidence in MSI images for a coherent fabric of lineations (grooves, ridges, squared-off crater walls [4]) may be inconsistent with a thorough rubble-pile, resulting from a subcatastrophic impact, although Eros' bulk density (~2.7 g/cc) suggests appreciable internal poros-

ity compared with that of hand-sample-sized L or LL chondrites.

Impact craters 0.1 to 1 km diameter have the same "empirical saturation" densities observed for craters of those sizes on Mathilde [5] and Ida [6] (but higher than for Gaspra). Some areas on Eros are deficient by 10 $\times$  in such craters, reflecting a localized process of crater erasure that has acted since most of the cratering occurred (while Eros still resided in the main asteroid belt). The numbers of smaller asteroidal projectiles inferred, e.g., from lunar craters imply that Eros should be saturated with still smaller craters, but it is not. In at least some cratered terrains, craters smaller than 100 m are progressively depleted (~10 $\times$  at 20 m diameter). Indeed boulders outnumber craters at sizes <20 m. These surprising observations raise questions about the nature of the pervasive, deep, impact-generated regolith expected on Eros. It is difficult to believe that smaller craters never formed, but what could have covered them up? An understanding of the genesis of the pervasive boulders, perhaps from systematic mapping of where they are concentrated vs. absent, would elucidate these issues (are they being exhumed from the bedrock of Eros, or are they crater ejecta/moonlets that have gently reaccreted onto Eros' surface?).

**Discussion:** In order to interpret Eros' infrared spectrum as well as its impact history, we must consider Eros' current environment and its dynamical history. Eros is subject to chaotic dynamics, so its past (and future) history is indeterminate. But probabilistic calculations [7] imply that Eros probably spent a long time in the asteroid belt, before evolving into its present orbit. While in its present orbit (for perhaps ~50 m.y.), its impact rate with main-belt projectiles may have been comparable with main-belt rates but probably was much lower (as low as ~1%).

If Eros' dynamical isolation from the main belt precluded any significant cratering (while fresh craters like Azzurra continued to form on Ida), space-weathering processes (some of which could modify spectra very quickly, cf. [8]) may have reached maturity while cratering was nil, explaining Eros' spectral blandness compared with Ida. Prominent, bright albedo patches on some steep slopes may indicate ongoing geological "readjustments"; very small craters could conceivably be covered up by active geological processes during the era of low cratering rates.

**References:** [1] Chapman C. R. (1996) *MAPS*, 31, 699–725. [2] Trombka J. I. et al. (2000) *Eos Trans. AGU*, 81, S287. [3] Veverka J. et al. (2000) *Science*, submitted. [4] Prockter L. et al. (2000) *Eos Trans. AGU*, 81, S286. [5] Chapman C. R. et al. (1999) *Icarus*, 140, 28–33. [6] Chapman C. R. et al. (1966) *Icarus*, 120, 77–86. [7] Michel P. et al. (1998) *Astron. J.*, 116, 2023–2031. [8] Hapke B. (2000) *LPS XXXI*, Abstract #1087.

**RHENIUM-OSMIUM FRACTIONATION IN GROUP IIIAB IRON METEORITES.** J. H. Chen<sup>1</sup>, D. A. Papanastassiou<sup>1,2</sup>, and G. J. Wasserburg<sup>1</sup>, <sup>1</sup>Charles Arms Laboratory, Division of Geological and Planetary Sciences, California Institute of Technology, Pasadena CA 91125, USA (jchen@gps.caltech.edu), <sup>2</sup>Division of Earth and Space Sciences, Jet Propulsion Laboratory, Pasadena CA 91109, USA.

Group IIIAB is a large iron meteorite group, showing compositional trends suggestive of formation by extensive fractional crystallization of a magma. However, there are problems in explaining some key IIIAB trends using simple fractional crystallization models and published partition coefficients. We analyzed Re, Os in members of the low-Ir (<0.1 ppm) IIIB subgroup. All IIIAB data are consistent with a single isochron and with the IIAB isochron [1,2]. In contrast to low-Ir pallasites, the high-Ni and low-Ir IIIAB irons show a limited range in <sup>187</sup>Re/<sup>188</sup>Os (0.57–0.60). In a log[Os]-log[Re] diagram (Fig. 1, top), the high- and low-Ni IIIAB subgroups define two straight lines with different slopes, as observed also for IIAB irons [3]. In a log[<sup>187</sup>Re/<sup>188</sup>Os]-log[Re] diagram (Fig. 1, bottom), our new data substantially extend the range for low-Re IIIAB irons (A = Acuna, BR = Bella Roca, Ch = Chupaderos, and G = Grant) and those from the literature (G<sub>w</sub> = Grant, and TC<sub>w</sub> = Tieraco Creek) [3–5]. We also show the IIAB data [3]. We note that both for IIAB and IIIAB there is a discontinuity in the curves shown, as addressed, in detail, for the IIAB by Morgan et al. [3]. The trends for Re/Os for Re > ~0.1 ppm (~50% FeNi crystallization), follow a simple fractional crystallization model with different but constant Re and Os partition coefficients [3]. We observe the following: (1) The slopes of the lines (for Re > 0.1 ppm) and the total range of Re/Os fractionation for IIIAB and IIAB are different, as the IIIABs show a shallower slope and a smaller range of fractionation than the IIABs;

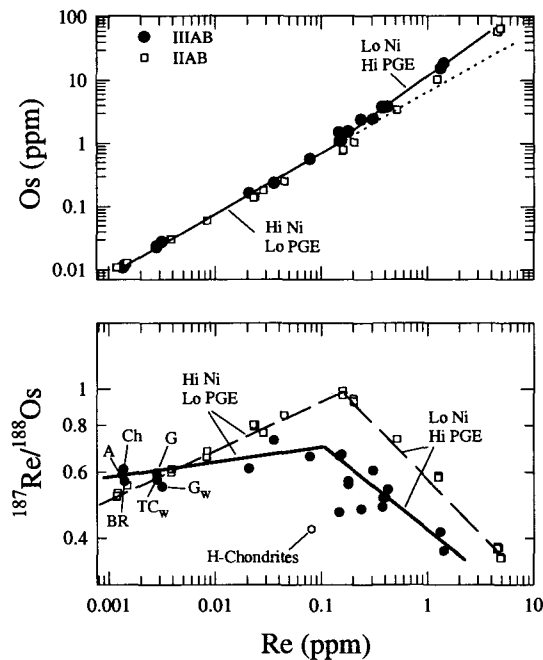


Fig. 1.

(2) the high-Ni IIIAB irons ( $\text{Re} < 0.1$  ppm) show essentially a constant  $\text{Re}/\text{Os}$ , over  $\sim 2$  orders of magnitude in  $[\text{Re}]$ ; and (3)  $^{187}\text{Re}/^{188}\text{Os}$  for IIIABs with  $\text{Re} < 0.1$  ppm is distinctly higher than for H6 chondrites ( $^{187}\text{Re}/^{188}\text{Os} = 0.423 \pm 0.007$ ) [6]. It is difficult to explain the discontinuity in the evolution of the fractionation trends for  $\text{Re}/\text{Os}$ . The IIIAB suggest that the relative partition coefficients for Re and Os shift to nearly equal values. The data for the high-Ni, low-Re IIIABs are not consistent with contamination with unfractionated (chondritic) material, but are instead suggestive of inclusion of Re and Os whose relative proportions were established in the magma prior to extreme depletion.

On Ir-Au and Ir-As diagrams, IIIAB irons form broad bands that have been interpreted as due to the trapping of parental magma within the crystallizing solids [7]. In this model, BR and Ch have high S contents and plot close to the liquid tracks of the IIIAB Ir-Au or Ir-As compositional fields (after  $\sim 78\%$  crystallization of the IIIAB core). Grant has moderate S and plots between the solid and liquid tracks (after  $\sim 75\%$  crystallization). The limited range in  $\text{Re}/\text{Os}$  in these three IIIAB samples is consistent with the calculated small differences in the degree of crystallization (75–78%), but still requires minor  $\text{Re}/\text{Os}$  fractionation, for  $\text{Re} < 0.1$  ppm.

**References:** [1] Chen et al. (2000) *LPS XXXI*, Abstract #1505. [2] Shen et al. (1996) *GCA*, 60, 2887. [3] Morgan et al. (1995) *GCA*, 59, 2331. [4] Morgan et al. (1992) *EPSL*, 108, 191. [5] Walker et al. (1993) *LPS XXIV*, Abstract #1477. [6] Chen et al. (1999) *GCA*, 62, 3379. [7] Wasson J. T. (1999) *GCA*, 63, 2875.

#### THE DIFFERENT FORMATION PROCESS BETWEEN L/LL AND ENSTATITE CHONDRITES.

J. Chikami<sup>1</sup> and M. Miyamoto<sup>2</sup>, <sup>1</sup>Senshu University, Higashi-Mita 2-1-1, Tama-ku, Kawasaki-shi, Kanagawa 214-8580, Japan (chikami@isc.senshu-u.ac.jp), <sup>2</sup>Mineralogical Institute, University of Tokyo, Hongo 7-3-1, Bunkyo-ku, Tokyo 113-0033, Japan (miyamoto@eps.s.u-tokyo.ac.jp).

**Introduction:** We proposed that Zn content in spinel-structured minerals might be an indicator for differentiation process in the early solar system [1]. A recurring theme is the possibility that there are significant compositional differences among petrologic type of a single chondrite group. Sears

and Weeks [2] concluded that abundances of siderophile elements increase with higher petrologic type between H and L chondrites.

From our recent study it has been found that ZnO contents in L/LL chromites do not show any trend over different petrologic type [3]. On the other hand, enstatite chondrites showed that Zn content in daubreelite decreases from lower to higher petrologic types [3]. In both L/LL and enstatite chondrites, bulk Zn content is almost constant over different petrologic type [4,5]. Different Zn behavior between L/LL and enstatite chondrites suggests their different formation process.

**Result:** We showed ZnO wt% for chromites in L4–L6 and LL4–LL7 and Zn wt% for daubreelites in EH3–EH4 using EPMA (15 kV, 12 nA, and Bence-Albee correction for chromites and 15 kV, 24 nA, and ZAF for daubreelite) (the detection limit of ZnO/Zn is 0.01 wt%): L4: Y 81070 (0.30–0.53), Y 791710 (0.41–0.62), Y 791630 (0.59), Y 791635 (0.44–0.64); L5: Y 790723 (0.10–0.19); L6: Y 75102 (0.29–0.58), Y 82178 (0.30–0.49), ALH 77269 (0.30–0.45); LL4: Y 791668 (0.32–0.48), Y 792772 (0.15–0.45); LL5: Asuka 87251 (0.15–0.28); LL6: Y 793506 (0.31–0.42), Y 75258 (0.15–0.30); LL7: Y 74160 (0.6), Y 82067 (0.2–0.3); EH3: ALH 77295 (4.0–5.0), Y 74370 (2.3–3.5), Qingzhen (4.0–8.0); EH4: St. Marks (0.6–1.2), Kaidun (0.06–0.11), Indarch (–0.1).

**Discussion:** Zhang et al. [6] suggested that none of the compositional trends in highly volatile elements observed for the ordinary chondrites are present in enstatite chondrites. In contrast to the above observation on bulk Zn content, the Zn content in daubreelite decreases with higher petrologic type in EH chondrites. We now consider three possible explanations for why the Zn content in daubreelite decreases with higher petrologic type although the bulk Zn content is similar: (1) an increase in  $f_{\text{O}_2}$  during equilibration, thus leading to incorporation of Zn into silicates as ZnO; (2) an increase in equilibrium temperature during equilibration, thus leading to change in partition coefficients between daubreelite and silicate; (3) a change in the number of daubreelite grains that are the main reservoir of Zn.

With the exception of highly volatile Br, no significant differences in abundance are observed among the petrologic types of the L/LL group [5,7]. This is consistent with our results that show no ZnO change over petrologic types in chromites of L/LL chondrites. Abundances of Cu and Zn in ordinary chondrites seem to have been mostly controlled by the nebular fractionation (not shock metamorphism and thermal metamorphism) [7].

Zinc behavior of spinel minerals in different petrologic types distinguished ordinary chondrites from enstatite chondrites. In enstatite chondrites many elements less volatile than Bi, Tl, or In are correlated [8]. On the other hand, in unequilibrated ordinary chondrites the seven elements Ag to Zn exhibit only three relationships (Al and Tl, Cs and Bs, S and In) [8]. This would suggest that if metamorphism affected ordinary chondrites, particularly the unequilibrated ones, it was much more subtle than that involved in enstatite chondrites.

**Conclusions:** Different Zn behavior shows that formation of L/LL chondrites apparently involved a more subtle thermal process than affected enstatite chondrites.

**References:** [1] Chikami J. et al. (1999) *Antarct. Meteorite Res.*, 12, 139–150. [2] Sears D. W. G. and Weeks K. S. (1986) *GCA*, 50, 2815–2832. [3] Chikami J. (1999) Ph.D. thesis, Univ. of Tokyo, 110 pp. [4] Kallemeyn G. W. and Wasson J. T. (1986) *GCA*, 50, 2153–2164. [5] Kallemeyn G. W. et al. (1989) *GCA*, 53, 2247–2767. [6] Zhang Y. et al. (1995) *JGR*, 100, 9417–9438. [7] Ebihara M. et al. (1993) *Meteoritics*, 28, 343. [8] Binz C. M. (1976) *GCA*, 40, 59–71.

#### FORMATION OF AMOEBOID OLIVINE INCLUSIONS IN CO3.0 CHONDRITES BY MELTING IN THE SOLAR NEBULA.

L. J. Chizmadia<sup>1</sup>, A. E. Rubin<sup>2</sup>, and J. T. Wasson<sup>1,2</sup>, <sup>1</sup>Department of Earth and Space Sciences, University of California, Los Angeles CA 90095-1567, USA, <sup>2</sup>Institute of Geophysics and Planetary Physics, University of California, Los Angeles CA 90095-1567, USA.

Amoeboid olivine inclusions (AOI) are fine-grained, irregularly shaped 100–500- $\mu\text{m}$  objects that constitute 8–16 vol% of CO chondrites [1]. The best-preserved AOI are found in CO3.0 chondrites (ALHA77307, Y 81020, Colony). The AOI are composed (in vol%) of 65% forsterite, 14% anorthite, 14% Ti-bearing diopside, and 7% metallic Fe-Ni. They also contain small (1–